

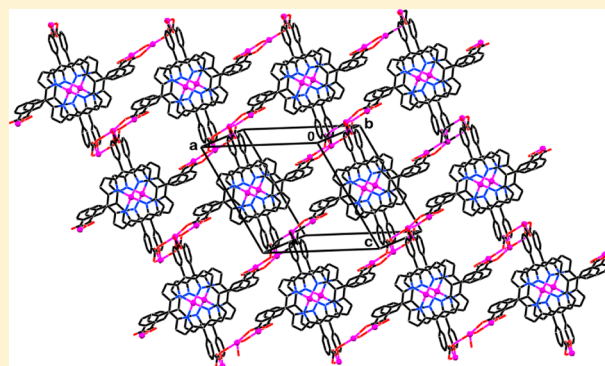
# Supramolecular Crystal Chemistry with Porphyrin Tinkertoys. Hydrogen-Bonding and Coordination Networks with the “Chair” and “Table” Conformers of Tetra(3-carboxyphenyl)porphyrin

Sophia Lipstman and Israel Goldberg\*

School of Chemistry, Sackler Faculty of Exact Sciences, Tel-Aviv University, 69978 Ramat-Aviv, Tel-Aviv, Israel

## Supporting Information

**ABSTRACT:** This study explores further the supramolecular reactivity of the *meso*-tetra(3-carboxyphenyl)porphyrin ( $T^3CPP$ ) building block in the context of crystal engineering.  $T^3CPP$  has coordination as well as hydrogen bonding tetradentate functionalities, and exhibits orientational versatility of the 3-carboxylic substituents with respect to the porphyrin core; chair- and table-like conformers have been expressed in this study. In the “chair” variant of  $T^3CPP$ , two adjacent carboxylic functions are oriented upward and the other two downward, while in the “table” isomer all four carboxylic arms are oriented in the same direction. Solvothermal reactions of the  $T^3CPP$  with cadmium and zinc ions afforded metalation of the porphyrin core and hybrid coordination compounds with uniquely interesting and novel architectures. This includes a discrete 4:2 Cd/Zn:porphyrin assembly (4), where the four metal ions link (as mononuclear connectors) between the two metalloporphyrins (present in a “table” conformation) into a molecular-box, as well as coordination polymers of one-dimensional (5) and two-dimensional (6–8) connectivity. Additional experiments led to the syntheses of hydrogen-bonded networks between the  $T^3CPP/Co-T^3CPP$  moieties (given in the “chair” conformation) and various amine ligands present in the reaction mixtures (1–3). These were associated with either partial or full proton-transfer from the porphyrin tetra-acid to the amine species to further stabilize the supramolecular networking by added electrostatic attraction. The above findings confirm that the  $T^3CPP$  scaffold may effectively engage in diverse supramolecular constructs, through direct multiple-coordination to metal-ion connectors, as well as in extended hydrogen-bonding networks. While the occurrence of the “table” conformer of  $T^3CPP$  in the above context has been observed here for the first time, new supramolecular materials are expected to emerge in the future with the still missing tetrahedral form (with the carboxylic substituents oriented in alternating directions around the porphyrin macrocycle) of this versatile ligand.



## INTRODUCTION

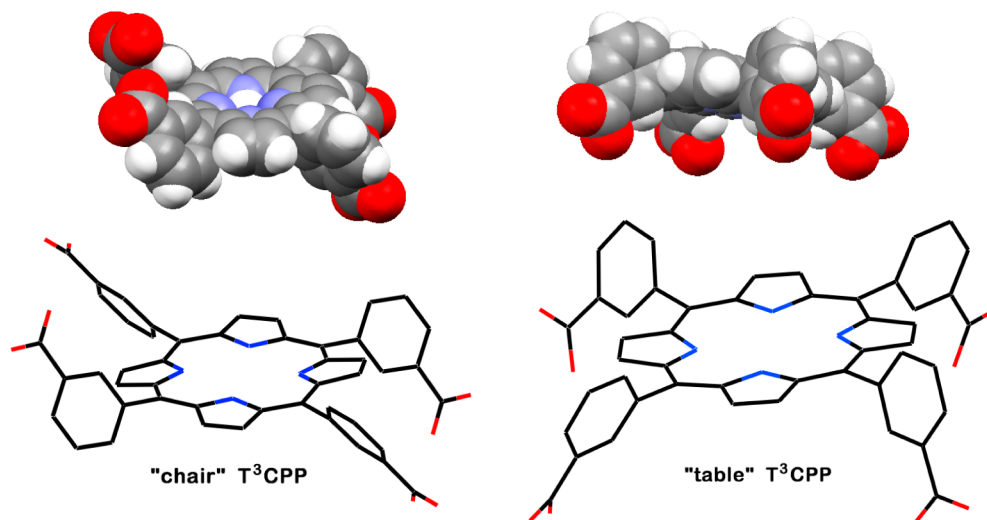
*meso*-Carboxyphenylporphyrins turned out to be an almost inexhaustible source of building blocks for the formulation of either hydrogen-bonding or coordination-driven (also with the aid of exocyclic metal-ion connectors) supramolecular assemblies, revealing an extraordinarily rich molecular recognition capacity. They exhibit a high tendency to involve through their peripheral  $-COOH$  sites in self-assembly processes, yielding readily multiporphyrin networks and frameworks in crystalline solids of varying topology and dimensionality. Possible metalation of the porphyrin core adds yet another dimension to the binding ability of this ligand along the equatorial and axial directions. Our pioneering demonstration of these unique features in the context of crystal engineering concerned the *meso*-5,10,15,20-tetra(4-carboxyphenyl)porphyrin scaffold in the free-base and metalated forms ( $T^4CPP$  and  $M-T^4CPP$ , respectively), and their networking into homomolecular and heteromolecular (with other organic as well as inorganic partners) assemblies of fascinating open architectures.<sup>1–4</sup> The intrinsic rigidity and

bulkiness of this porphyrin framework, associated with its multidentate and multidirectional binding functionality (utilizing either the neutral or the deprotonated forms of the carboxylic functions), provide excellent potential for the construction of porous framework solids. Consequently, it has been shown by Suslick et al. that hybrid organic( $T^4CPP$ )-inorganic(metal-ion-connectors) porous coordination polymers can be utilized in selective sorption of molecular guest components into the crystalline lattice.<sup>5–7</sup> It further emerged that polynuclear metal-ion moieties (instead of single ions) provide more robust and more effective connectors in formulations of porous porphyrin-based solids. Following these early findings, a large number of  $T^4CPP$ -based coordination networks with a variety of transition metal ions have been synthesized by us and others, as summarized in a series of review-type papers.<sup>8–10</sup> More recent work involves

Received: November 25, 2012

Revised: December 30, 2012

Scheme 1. Wireframe (Connectivity) and Space-Filling (Molecular Shapes) Illustrations of the Chair- and Table-Like Conformers of the T<sup>3</sup>CPP [*meso*-5,10,15,20-Tetra(3-carboxyphenyl)porphyrin] Scaffold Differing in Relative Orientations of the Carboxyphenyl “Legs”



porous framework solids composed of the T<sup>4</sup>CPP linkers and pillared lanthanoid ion connectors,<sup>11</sup> tunable heterometallic frameworks constructed from paddle-wheel secondary building units and with open metal centers (this feature could be particularly useful for heterogeneous catalysis applications),<sup>12–16</sup> and materials active for visible-light catalysis.<sup>17</sup> Another recent development involves the formation of hybrid T<sup>4</sup>CPP-metal frameworks not only in crystalline bulk but also as highly crystalline nanofilm on surfaces.<sup>18</sup> In a similar context, further interest was drawn at the synthesis of microporous framework solids and functional materials with other carboxyphenylporphyrin linkers as well. Outstanding recent examples involve organic scaffolds bearing either two (trans-related) or four 3,5-dicarboxyphenyl functions at the *meso* positions of the porphyrin macrocycle.<sup>19,20</sup> The latter was found to self-assemble with zinc and cadmium ions, through its eight carboxylic recognition groups, yielding permanently microporous materials with selective CO<sub>2</sub> uptake. Numerous examples of other coordination polymers involving porphyrin building blocks with either two or three 4-carboxyphenyl substituents have also been reported.

During our continuing crystal engineering investigations of porphyrin-based framework solids, we decided to explore also the use of the tetra(3-carboxyphenyl)porphyrin building block (T<sup>3</sup>CPP) to this end, as this ligand has similar tetradentate functionality and molecular recognition potential to that of the widely explored T<sup>4</sup>CPP isomer. The main difference between the two ligands is in the substitution pattern of the peripheral carboxylic acid groups. The T<sup>4</sup>CPP derivative of approximate *D*<sub>4h</sub> symmetry is characterized by one main conformation with the COOH-sites directed at the four equatorial positions of the porphyrin entity. The disposition of the carboxylic acid functions in T<sup>3</sup>CPP is more versatile, as each one of them can point either up or down with respect to the central core, thus potentially enhancing the three-dimensional connectivity features of this unit and the variety of the supramolecular aggregates it may form. Thus, the T<sup>3</sup>CPP ligand can appear in one out of four main different conformations. In the “chair” conformer two *syn*-related carboxyphenyl rings are oriented upward and the other two downward. In the “tetrahedral”

structure, the adjacent COOH groups around the porphyrin macrocycle point alternately either up or down. In the “table” conformer all four carboxylic acid functions (“legs”) are aligned in the same direction in relation to the porphyrin ring. The remaining “throne-like” structural form is characterized by one carboxyphenyl group pointing down and the other three pointing up. In an earlier investigation the successful synthesis of framework hybrid coordination polymers composed of T<sup>3</sup>CPP (as well as of the analogous) T<sup>4</sup>CPP species and various lanthanoid metal ions has been demonstrated.<sup>21</sup> In all structures reported therein, the continuous coordination schemes with the T<sup>3</sup>CPP tetra-acid (in deprotonated form to suitably account for charge balance in the metal-coordinated ensembles) involved the ligand in a “chair” form, which favors the formation of extended connectivity patterns in three dimensions. Recent crystal-engineering investigations of coordination networks with the tetra(3-pyridyl)porphyrin building block (T<sup>3</sup>PyP) and transition metal ions also revealed that this ligand adopts frequently the chairlike conformation.<sup>22,23</sup> Yet, it has been shown further in that study that when metallic nodes with inherent tetrahedral coordination environment are used in the supramolecular synthesis, they interact preferentially with the tetrahedral conformer of T<sup>3</sup>PyP to construct diamondoid framework materials. The “table” and “throne” forms of T<sup>3</sup>PyP were not observed in crystals thus far.

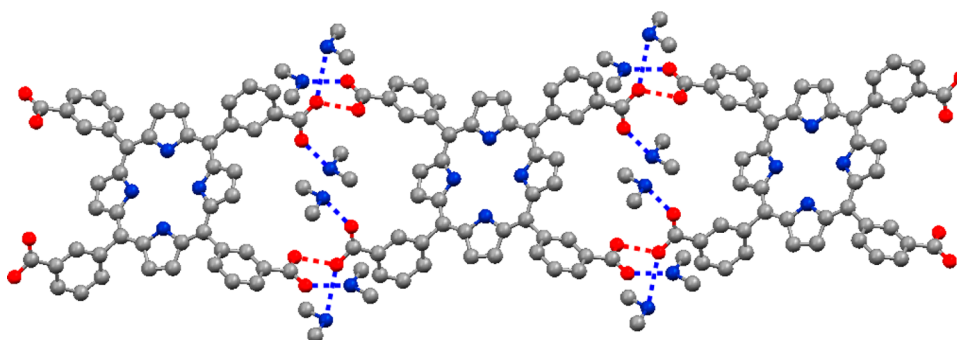
In light of the above observations, the present work evaluates further the reactivity of T<sup>3</sup>CPP and its conformationally versatile synthons of supramolecular interaction with other components, and we report here on the preparation and structural characterization of a series of new T<sup>3</sup>CPP-derived materials. This includes elucidation of the ammonium salts of the freebase and Co-metalated ligand (obtained as byproducts of the synthesis of coordination materials), and its coordination polymers of zero, one-, and two-dimensional connectivity with *d*-transition metals (Cd and Zn). The newly analyzed compounds include the hydrogen-bonded assemblies (associated with proton transfer from the porphyrin to the amine) of the freebase T<sup>3</sup>CPP with dimethylamine (**1**); and 1,8-diazabicyclo[5.4.0]undec-7-ene (DBU) (**2**); as well as of Co-T<sup>3</sup>PyP with dimethylamine and aqueous ammonia (**3**). In these

Table 1. Crystal and Experimental Data for Structures 1–8

	1 <sup>a</sup>	2	3	4
formula	C <sub>52</sub> H <sub>44</sub> N <sub>6</sub> O <sub>8</sub>	C <sub>66</sub> H <sub>62</sub> N <sub>8</sub> O <sub>8</sub>	C <sub>52</sub> H <sub>48</sub> CoN <sub>8</sub> O <sub>8</sub>	C <sub>178</sub> H <sub>140</sub> Cd <sub>6</sub> N <sub>24</sub> O <sub>20</sub>
<i>F</i> <sub>w</sub>	880.93	1095.24	971.91	3609.54
crystal system	triclinic	monoclinic	triclinic	monoclinic
space group	<i>P</i> $\bar{1}$	<i>P</i> 2 <sub>1</sub> / <i>c</i>	<i>P</i> $\bar{1}$	<i>P</i> 2 <sub>1</sub> / <i>c</i>
<i>a</i> [Å]	6.9563(3)	7.1066(7)	5.0617(2)	18.2876(3)
<i>b</i> [Å]	9.5096(6)	13.1551(12)	13.1465(4)	15.7800(3)
<i>c</i> [Å]	16.9966(9)	29.311(3)	17.5900(7)	29.0197(5)
$\alpha$ [°]	86.781(4)	90.0	81.733(2)	90.0
$\beta$ [°]	89.772(4)	91.769(3)	81.830(2)	108.5978(12)
$\gamma$ [°]	72.069(4)	90.0	83.744(3)	90.0
<i>V</i> [Å <sup>3</sup> ]	1067.95(10)	2738.9(4)	1141.89(7)	7937.1(2)
<i>Z</i>	1	2	1	2
$\rho_{\text{calcd}}$ [Mg m <sup>-3</sup> ]	1.370	1.328	1.413	1.510
$\mu$ [mm <sup>-1</sup> ]	0.765	0.089	0.443	0.865
<i>F</i> (000)	462	1156	507	3648
crystal size [mm <sup>3</sup> ]	0.08 × 0.03 × 0.02	0.31 × 0.08 × 0.03	0.20 × 0.20 × 0.15	0.35 × 0.25 × 0.10
$\theta_{\text{max}}$ [°]	66.53	26.19	27.85	25.05
refl collected	15947	16865	7125	51754
refl unique	3528	5459	3987	14029
<i>R</i> (int)	0.050	0.036	0.068	0.061
completeness (%)	94	99	100	100
refl with <i>I</i> > 2 $\sigma$ ( <i>I</i> )	2798	4134	3029	11190
refined parameters	301	370	331	1011
<i>R</i> <sub>1</sub> [ <i>I</i> > 2 $\sigma$ ( <i>I</i> )] <sup>b</sup>	0.046	0.055	0.055	0.061
<i>wR</i> <sub>2</sub> [ <i>I</i> > 2 $\sigma$ ( <i>I</i> )]	0.119	0.138	0.109	0.159
<i>R</i> <sub>1</sub> [all data] <sup>b</sup>	0.062	0.079	0.081	0.079
<i>wR</i> <sub>2</sub> [all data]	0.127	0.154	0.119	0.171
$\pm\Delta\rho_{\text{max}}$ [e Å <sup>-3</sup> ]	+0.30, −0.30	+0.53, −0.49	+0.43, −0.39	+1.95, −2.49
average C–C bond precision /Å	0.003	0.003	0.004	0.010
	5 <sup>b</sup>	6	7 <sup>b</sup>	8 <sup>b,c</sup>
formula	C <sub>68</sub> H <sub>44</sub> N <sub>8</sub> O <sub>8</sub> Zn <sub>3</sub>	C <sub>64</sub> H <sub>50</sub> Cd <sub>3</sub> N <sub>8</sub> O <sub>11</sub>	C <sub>57</sub> H <sub>49</sub> Cd <sub>3</sub> N <sub>8</sub> O <sub>12</sub>	C <sub>48</sub> H <sub>24</sub> Cd <sub>3</sub> Cl <sub>2</sub> N <sub>4</sub> O <sub>9</sub>
<i>F</i> <sub>w</sub>	1297.22	1433.59	1375.24	1208.82
crystal system	monoclinic	triclinic	triclinic	monoclinic
space group	<i>C</i> 2/ <i>c</i>	<i>P</i> $\bar{1}$	<i>P</i> $\bar{1}$	<i>P</i> 2 <sub>1</sub> / <i>m</i>
<i>a</i> [Å]	42.5453(5)	15.1307(2)	15.1052(5)	12.4017(6)
<i>b</i> [Å]	15.8928(3)	15.7557(3)	15.4349(5)	15.5770(13)
<i>c</i> [Å]	30.3631(5)	15.9818(4)	16.2932(7)	20.0534(17)
$\alpha$ [°]	90.0	92.47509(8)	94.0207(10)	90.0
$\beta$ [°]	129.3139(9)	117.4952(9)	117.5529(13)	104.298(6)
$\gamma$ [°]	90.0	115.0891(11)	114.1102(19)	90.0
<i>V</i> [Å <sup>3</sup> ]	15884.1(4)	2922.24(10)	2913.1(2)	3753.9(5)
<i>Z</i>	8	2	2	2
$\rho_{\text{calcd}}$ [Mg m <sup>-3</sup> ]	0.947	1.629	1.568	1.069
$\mu$ [mm <sup>-1</sup> ]	0.947	1.150	1.152	0.950
<i>F</i> (000)	5296	1433	1374	1180
crystal size [mm <sup>3</sup> ]	0.25 × 0.25 × 0.20	0.20 × 0.10 × 0.05	0.20 × 0.10 × 0.05	0.15 × 0.12 × 0.08
$\theta_{\text{max}}$ [°]	25.05	26.00	25.00	25.00
refl collected	46477	39645	27992	13006
refl unique	13930	11445	10222	6836
<i>R</i> (int)	0.091	0.066	0.071	0.098
completeness	100%	100%	100%	100%
refl with <i>I</i> > 2 $\sigma$ ( <i>I</i> )	9597	8409	7956	3101
refined parameters	784	791	713	147
<i>R</i> <sub>1</sub> [ <i>I</i> > 2 $\sigma$ ( <i>I</i> )] <sup>b</sup>	0.074	0.058	0.055	0.121
<i>wR</i> <sub>2</sub> [ <i>I</i> > 2 $\sigma$ ( <i>I</i> )]	0.176	0.161	0.115	0.310
<i>R</i> <sub>1</sub> [all data] <sup>b</sup>	0.105	0.086	0.077	0.196
<i>wR</i> <sub>2</sub> [all data]	0.187	0.177	0.122	0.342
$\pm\Delta\rho_{\text{max}}$ [e Å <sup>-3</sup> ]	+1.98, −2.12	+1.37, −1.15	+1.05, −0.85	+1.81, −0.88
average C–C bond precision /Å	0.009	0.012	0.010	0.018

Table 1. continued

<sup>a</sup>Measured with Cu K $\alpha$  radiation. <sup>b</sup>Excluding the solvent diffused within the interporphyrin channels: pyridine and methanol in **5** and DMF in **7** and **8** (see Experimental Section). <sup>c</sup>In **8** only the Cd and Cl atom were assigned anisotropic ADPs and the structural model is characterized by rather low precision.



**Figure 1.** Section of the hydrogen bonded supramolecular assembly in **1** (ball-and-stick illustration, the H-bonds being denoted by dashed lines). Note the zigzag chain-type association of the porphyrin units.

three compounds the porphyrin ligand adopts the chairlike structure (Scheme 1). Yet, in all the observed coordination polymeric structures the preferred geometry of the organic linker is table-like: discrete dimeric molecular box where two inverted T<sup>3</sup>CPP units are intercoordinated to one another (“legs-to-legs”) through cadmium-(COO<sup>2-</sup>)<sub>2</sub> binding synthons (**4**), one-dimensional chain of such molecular boxes where tetrahedral zinc ions provide for intra- as well as interbox connectors in one direction (**5**), Cd-bridged two-dimensional coordination layers where the Cd-ions tessellate the (T<sup>3</sup>CPP)<sub>2</sub> dimer and also bridge between adjacent dimers in two dimensions (**6** and **7**), and finally a different mode of “square-wave”-type coordination pattern of face-to-face-oriented in an offset manner T<sup>3</sup>CPPs interbridged by Cd-ions; the one-dimension “pipes” thus formed assemble into bilayered two-dimensional arrays through Cd–Cl<sub>2</sub>–Cd bridging units (**8**). The diverse topologies of the networks formed arise from competing coordination affinities to the metal centers of the carboxylic/carboxylate sites on the porphyrin and the auxiliary solvent moieties that occupy some of the coordination sites on the metal.

## RESULTS AND DISCUSSION

The fascinating supramolecular chemistry of the T<sup>4</sup>CPP ligand and its wide utility in diverse applications<sup>1–18</sup> encouraged us to examine the molecular recognition features of its closely related analogue T<sup>3</sup>CPP. This scaffold consists also of four divergent benzoic acid groups around the central porphyrin core, with high propensity to engage both in supramolecular hydrogen bonding as well as coordination synthons. The latter usually involve deprotonation of the acid functions and are considerably more robust; hence, their utility in the construction of microporous framework solids. In the previous study, we successfully demonstrated the formulation of hybrid coordination polymers by reacting T<sup>3</sup>CPP with lanthanoid-bridging ions in favorable hydrothermal conditions.<sup>21</sup> In these materials the tetradentate porphyrin units are intercoordinated by multinuclear assemblies of the bridging metal ions into open and thermally stable three-dimensional single-framework architectures. In order to facilitate and optimize bonding in all directions the functional carboxyphenyl substituent arranged in a “chair” conformation, with the two pairs oriented in

opposite directions with respect to the mean porphyrin plane. No other conformers of T<sup>3</sup>CPP have been observed in crystals thus far. Following our earlier findings with T<sup>3</sup>PyP-based coordination polymers (which revealed the occurrence of both the “chair” and “tetrahedral” conformers of the organic ligand), we reacted in this study the T<sup>3</sup>CPP ligand with various salts of selected d-metal ions, known of their preference for a tetrahedral coordination environment (e.g., Zn<sup>2+</sup> and Cd<sup>2+</sup>; see Experimental Section). It was anticipated that such exocyclic metal centers will favor the tetrahedral porphyrin functionality (with trans-related *m*-carboxyphenyl functions pointing up and the other two down with respect to the porphyrin plane), that may lead to the formation of coordination arrays of diamondoid topology. This work revealed, however, partly unexpected results. In many of these supramolecular syntheses, weak organic base (e.g., pyridine, DMF, DBU) was used as solubilizing environment in order to facilitate deprotonation of the porphyrin tetra-acid and interaction between the anionic linker and the metal reactant. Moreover, the DMF–water solvent environment has frequently been applied, as hydrolysis of the DMF (to dimethyl amine and formate anion) in hydrothermal conditions was found to promote the formation of metal organic frameworks.<sup>22</sup> However, in compounds **1–3** this resulted in hydrogen-bonding-driven self-assembly of the organic components associated with proton-transfer from the carboxylic acid to the basic solvent, instead of the desired porphyrin–metal coordination. The T<sup>3</sup>CPP moiety preserved the chairlike conformation in these structures. Then, while the crystal structures of the other products **4–8** are indeed dominated by metal–ligand coordination, somewhat surprisingly they were found to contain solely the “table” conformer of T<sup>3</sup>CPP (the tetrahedral conformer of this ligand has not been observed, as yet). In **4–8** the coordination occurs between the carboxylate “legs” of adjacent oppositely (legs-to-legs) oriented ligands, manifesting predominantly a molecular-box motif of metal-intercoordinated porphyrin dimer (see below). Further side-coordination of such molecular boxes through the same metal-ion centers creates a one-dimensional chain and two-dimensional layer motifs. The eight new crystalline products of the T<sup>3</sup>CPP/MT<sup>3</sup>CPP-based supramolecular assemblies (**1–8**) were

Table 2. Hydrogen-Bonding Parameters in 1–3<sup>a</sup>

O/NH (donor D)	O (acceptor A)	O/N–H (Å)	H...A (Å)	D...A (Å)	D–H...A (deg)
<b>1</b>					
OH20	O29 ( $x, y, z + 1$ )	0.84	1.66	2.481(2)	164
NH31a	O20 ( $x, y, z - 1$ )	0.92	2.22	2.978(2)	140
NH31b	O21 ( $x - 1, y, z - 1$ )	0.92	1.86	2.774(3)	168
<b>2</b>					
OH21	O29 ( $x, 1/2 - y, 1/2 + z$ )	0.84	1.68	2.509(2)	170
NH32	O30 ( $1 - x, y - 1/2, 1/2 - z$ )	0.88	1.94	2.798(3)	163
<b>3</b>					
NH31a	O30 ( $-x, -y, 1 - z$ )	1.00	1.85	2.837(4)	172
NH31b	O30 ( $1 - x, -y, 1 - z$ )	0.87	2.00	2.860(4)	169
NH31c	O29 ( $x, y, z - 1$ )	1.06	1.73	2.787(3)	171
NH31d	O21	0.95	1.83	2.768(4)	170
NH32a	O20	0.92	1.82	2.726(4)	167
NH32b	O21 ( $1 - x, 1 - y, -z$ )	0.92	1.85	2.748(4)	165

<sup>a</sup>O–H...O interactions are between adjacent porphyrin moieties, while NH...O bonds involve ammonium ions as proton donors and porphyrin units as proton acceptors.

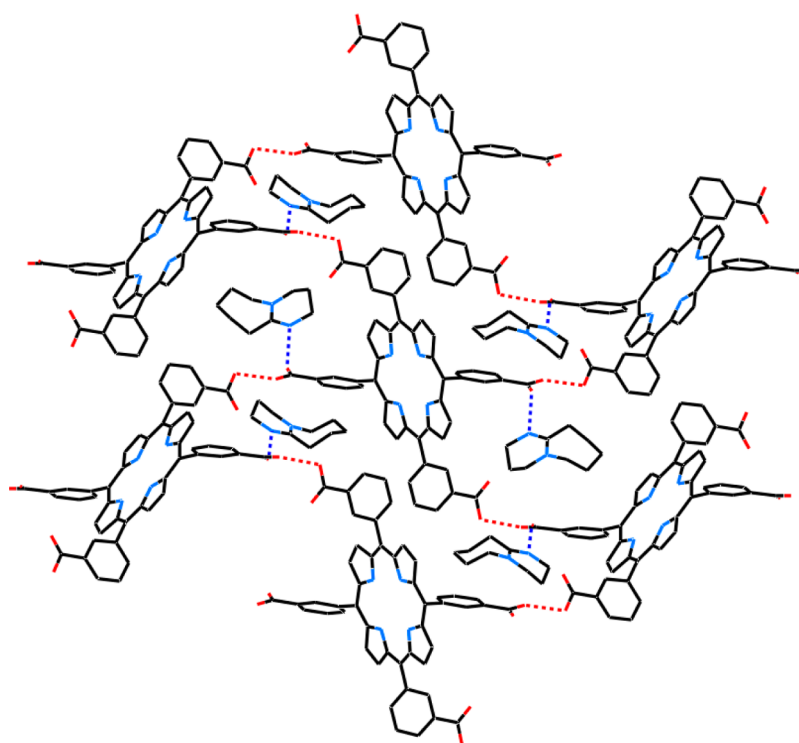


**Figure 2.** Wireframe illustration of the layered intermolecular organization in **2**, viewed down the  $a$ -axis of the crystal. The H-bonds are marked by dotted lines. Note that each porphyrin entity binds to four neighboring T<sup>3</sup>CPP units.

characterized by single-crystal X-ray diffraction. The crystallographic and experimental data are given in Table 1.

Crystal structures 1–3 are characterized by extended COOH...COO<sup>−</sup> and/or NH<sup>+</sup>...COO<sup>−</sup>/COOH hydrogen-bonding which propagates in two/three dimensions throughout the corresponding crystals. Figure 1 illustrates the supramolecular interaction pattern in **1**. Here the T<sup>3</sup>CPP (residing on inversion) cocrystallized with 2 equiv of dimethylamine (obtained from hydrolysis of DMF in the given reaction conditions). The intermolecular hydrogen-bonding capacity of these components was enhanced by double deprotonation of the porphyrin and corresponding protonation of the two amine moieties, as well as by the thus induced charge-assisted nature of the resulting bonds. The structure can be best described as

composed of hydrogen-bonded zigzag chains of T<sup>3</sup>CPP aligned along the  $c$ -axis of the crystal, where every unit is connected to two adjacent ones by four COOH...COO<sup>−</sup> bonds. The two “upper” COOH and COO<sup>−</sup> functions of one molecule associate with two “lower” COOH/COO<sup>−</sup> legs of an adjacent species. Such chains are arranged in the triclinic crystal parallel to each other and are further NH<sup>+</sup>...COO<sup>−</sup>/COOH interconnected along the sideways directions through the dimethylammonium ions (Table 2).

Crystals of **2** of similar 1:2 T<sup>3</sup>CPP/amine composition were obtained in the presence of the DBU non-nucleophilic base. As in the previous example, the tetra-acid ligand is doubly deprotonated with proton-transfer to the DBU species. However, in this case every T<sup>3</sup>CPP unit is COOH...COO<sup>−</sup>

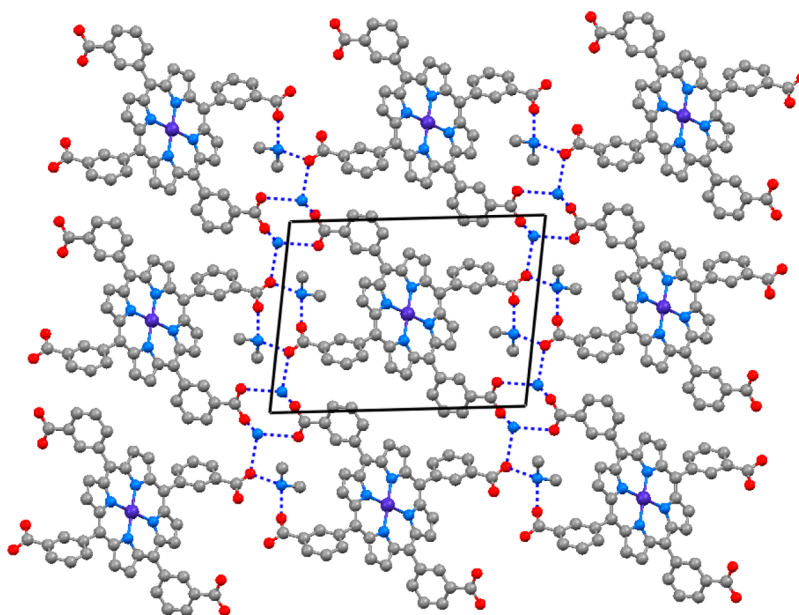


**Figure 3.** Section through the structure of **3** viewed down the *a*-axis of the unit-cell, and depicting part of the hydrogen bonding links (dotted lines) between the  $(T_3CPP)^+$ ,  $(CH_3)_2NH_2^+$ , and  $NH_4^+$  component species.

hydrogen-bonded to four different porphyrin moieties. Its carboxylate functions further associate with the two monoprotonated ammonium ions (Table 2). This results in the formation of two-dimensional hydrogen-bonded layers of corrugated surface, within which neighboring porphyrin units are oriented in a herringbone fashion. The layers are aligned parallel to the *bc* plane of the unit-cell, with the ammonium ions accommodated in a pillared manner within interporphyrin channel voids along the *b*-direction (Figure 2). Tight stacking of the layered assemblies along the *a*-axis completes the crystal packing of this structure. The above two structures consist of freebase  $T^3CPP$ s, as the large size of the cadmium(II) ion (0.97 Å) does not favor its full insertion into the porphyrin core ( $Zn^{2+}$  with an ionic diameter of 0.74 Å fits best an undistorted core).

On the other hand, metalation of the porphyrin macrocycle with the smaller cobalt ions seems considerably easier. Moreover, the presence of a stronger ammonium hydroxide base in the reaction mixture of **3** resulted in complete deprotonation of the  $Co-T^3CPP$  moiety. The latter cocrystallized, correspondingly, with 2 equiv of dimethylammonium and 2 equiv of ammonium cations, which act as hydrogen bonding bridges (Table 2) between the porphyrin units in the structure. The entire crystal structure can be described as composed of parallel columns of offset-stacked porphyrin entities aligned along the *a*-axis cross-linked to one another in three dimensions by the two types of ammonium ions (Figure 3). In the above three examples both the freebase and metalated variants of the porphyrin moiety were found to adopt the chairlike conformation (Scheme 1), with either partial or full solvation of the carboxylic/carboxylate groups.

It has become obvious at this stage that different solubilizing conditions are needed for a successful synthesis of coordination-driven polymeric compounds, avoiding as much as possible hydrolysis of DMF and the use of strong basic reagents. Crystallization mixtures of DMF/ethanol/methanol/pyridine turned out to provide more favorable conditions to this end.

Structure **4** reveals a unique and previously unobserved “molecular-box”-type assembly mode, where the  $T^3CPP$  adopts a “table” conformation with all the carboxylate legs directed in the same direction with respect to the porphyrin plane (Figure 4). In this reaction, metallation of the porphyrin core has

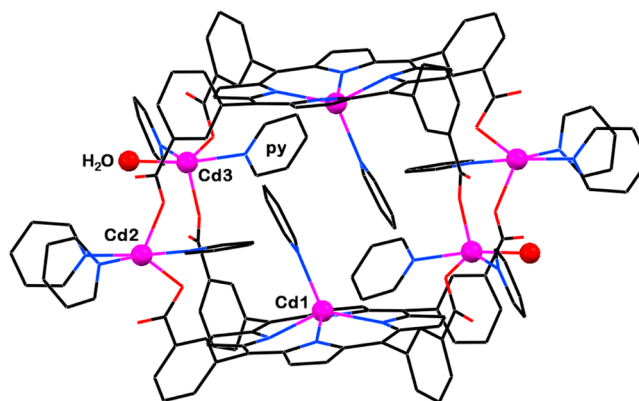


**Figure 4.** The discrete (0-D) molecular-box-type coordination assembly in **4** that involves two table conformers of  $Cd-T^3CPP$  tessellated into a box-type dimer by four  $(COO^-)-Cd-(COO^-)$  coordination bridges. The Cd ions and water molecules are depicted by spheres. The five-coordinate environment of the  $Cd2/Cd3$ -ions (either trigonal-bipyramidal or square-pyramidal) is supplemented by pyridine and water ligands. The  $Cd1-N_{pyrrole}$  and  $Cd1-N_{pyridine}$  coordination distances are 2.174–2.218(5) Å and 2.320(6) Å, respectively. The  $Cd2/Cd3-O_{carboxylate}$  bonds are within 2.233–2.280(4) Å.

occurred. The relatively large  $Cd^{2+}$  (ionic radius 0.97 Å) ( $Cd1$ ) is located in a perching position with respect to the four pyrrole rings. It is five-coordinate, with an additional axial pyridine ligand bound to it on the convex side. Then, four other cadmium ions ( $Cd2$ ,  $Cd3$ , and their inversion-related equivalents) connect by leg-to-leg coordination between two neighboring and inversion-related  $Cd1(pyridine)$ -porphyrin moieties oriented in opposite directions, to yield a molecular

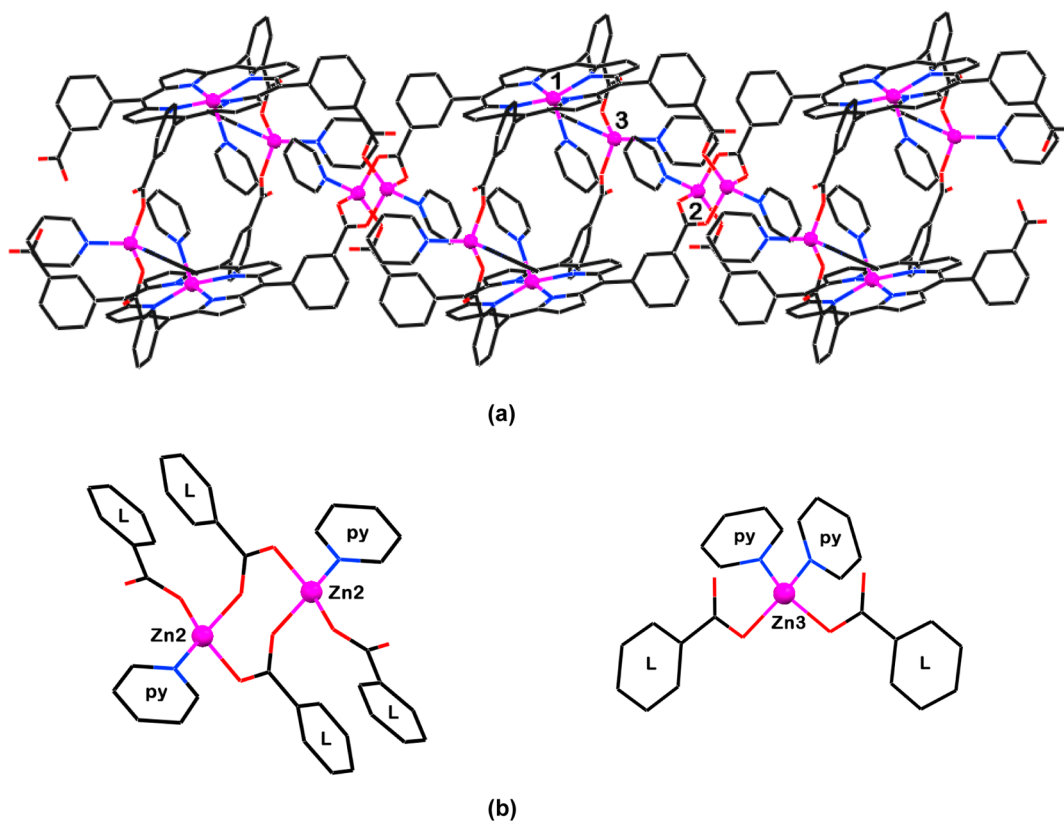


**Figure 5.** (a) The coordination chains in **5**, propagating along the *b*-axis of the crystal. The Zn1(py)-T<sup>3</sup>CPP entities associate into a molecular-box-type assembly via coordination synthons of two types as shown in (b): dinuclear (Zn<sub>2</sub>)<sub>2</sub>(py)<sub>2</sub>(COO<sup>-</sup>)<sub>4</sub> and mononuclear Zn<sub>3</sub>(py)<sub>2</sub>(COO<sup>-</sup>)<sub>2</sub> clusters. The former units (located on inversion) tessellate also the dimeric boxes into the 1D coordination-polymeric aggregate. In (b) the metal-coordinated Zn1(py)-T<sup>3</sup>CPP and pyridine ligands are marked by “L” and “py”, respectively.

box (Figure 4). In the latter all eight carboxylate functions turn inward, and its lower and upper faces are lined by the concave surfaces of the porphyrin core fragments. These additional Cd-ions reveal roughly a trigonal bipyramidal coordination environment. Three pyridines or two pyridines and one water molecule coordinate to these metal centers along the three equatorial directions, while two carboxylate arms of two different porphyrin units bind to them in a monodentate fashion along the *trans*-related axial directions. The former line the perimeter of thus formed molecular box. The inner space within the coordination porphyrin dimer is effectively filled with the axial pyridine ligands to the porphyrin-inserted ion (Cd1). Additional uncoordinated molecules of methanol and pyridine solvents fill the intermolecular voids in the crystal. The coordinated water and the methanol species take part in intermolecular hydrogen bonds.

The presence of pyridine in the crystallization mixture facilitated also the crystallization of compound **5** (where zinc ions were used instead of cadmium ions) in the form of single crystals, as otherwise this product could be obtained only in the form of a polycrystalline material. From the structure of **4** it could be deduced that pyridine plays an important function in stabilizing the molecular-box-type pattern, as in their role as an axial ligand to the metal inserted into the porphyrin core, they also fill the inner space inside the box.

As in the previous example, the Zn-T<sup>3</sup>CPP in **5** is five-coordinate and has a domed shape, the central zinc ion (Zn1) being coordinated to the four pyrrole N-atoms (at 2.070–2.090(4) Å), as well as to an axial pyridine ligand (at 2.145(4) Å) (Figure 5). The table-conformer is well expressed in this

structure too, with all the carboxylate functions of a given porphyrin moiety pointing in the same direction. Adjacent porphyrins related by inversion are intercoordinated via the zinc-ion nodes into a dimer assembly. The bridging zinc ions displaced around the perimeter, Zn2 and Zn3, are characterized by a tetrahedral coordination environment. Zn3 coordinates between two converging carboxylate residues from the upper and lower porphyrin units (each coordinated to the metal in a monodentate manner) and to two additional pyridine ligands on the periphery. However, in addition to the carboxylates from the upper and lower units in the overlapping porphyrin pair, only one pyridine ligand is coordinated to Zn2. The remaining coordination valency is utilized instead to coordinate to the carboxylate entity of a neighboring molecular box displaced along the *b*-axis by  $\pm b$ . This results in a formation of a dinuclear (Zn<sub>2</sub>)<sub>2</sub>(py)<sub>2</sub>(COO<sup>-</sup>)<sub>4</sub> coordination synthon where two of the carboxylate units bridge between the two metal ions in chelating bidentate fashion, the other two carboxylates linking in a monodentate mode (Figure 5b). All the above Zn–O<sub>carboxylate</sub> and Zn–N<sub>pyridine</sub> coordination bonds range from 1.972(4) to 2.039(5) Å. The Zn2...Zn2 distance between the inversion-related metal ions in the dinuclear connector is 3.869(2) Å. This links the dimer units into a one-dimensional coordination polymer. In the crystal, the polymeric chains propagate along the *b*-axis and align parallel to one another, molecules of the solvent filling the interstitial voids between them.

Further attempts led to polymeric products of higher dimensionality than in **4** (discrete coordination box) and **5** (one-dimensional coordination chain of such boxes). The

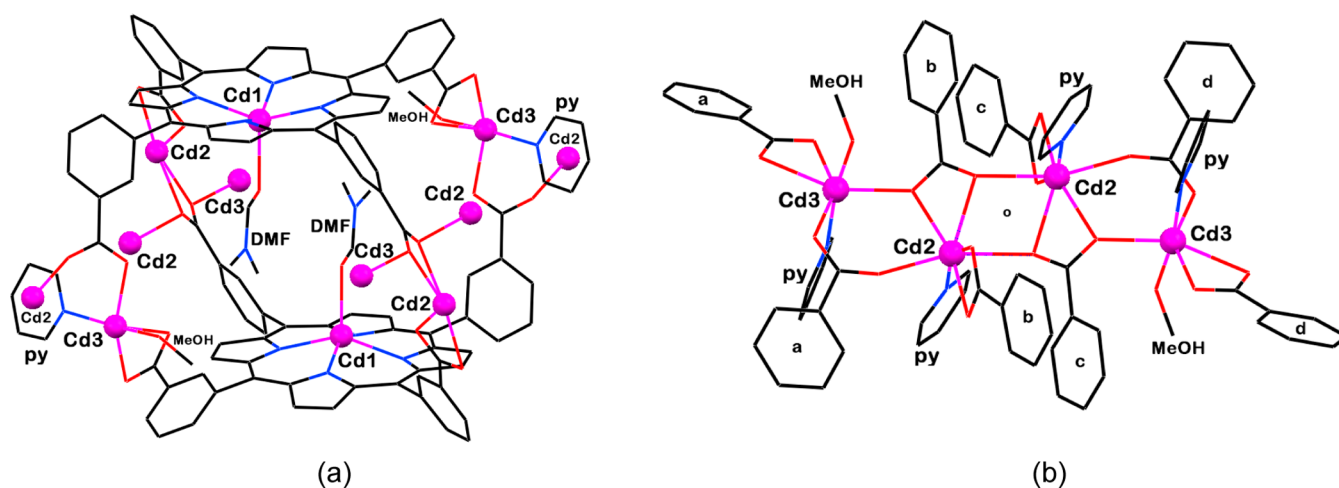


**Figure 6.** (a) The molecular-box motif in **6**. For clarity some of the pyridine species linked to Cd2 and Cd3 are omitted. (b) The tetranuclear coordination synthon operative at the four bridging sites around a given molecular box. Each of the metal ions connects to the two porphyrin faces in a molecular box (the two coordinating carboxylates of a given box are marked by either a, b, c, or d) as well as to the porphyrins of adjacent boxes. The Cd2...Cd2 and Cd2...Cd3 distances within the tetranuclear clusters are 3.893(2) and 3.999(2) Å.

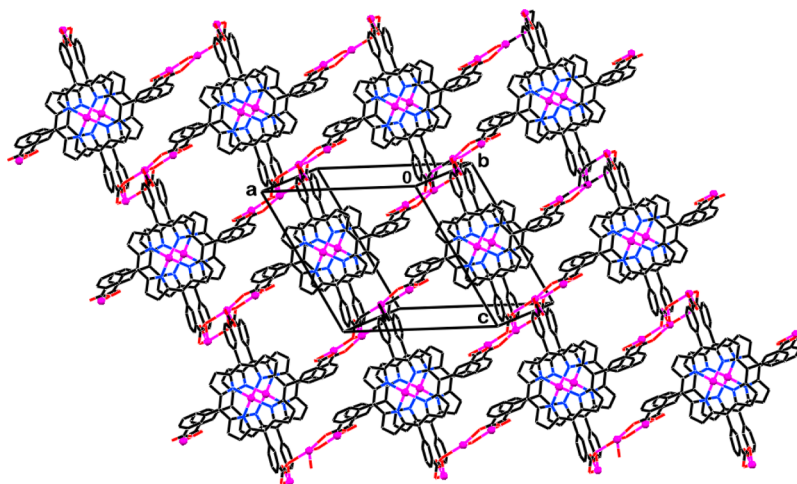


**Figure 7.** Perspective view, approximately down the *b*-axis, of the bilayered two-dimensional coordination polymer in **6** and **7**. For clarity the auxiliary pyridine and DMF ligands are not shown. Note the repeating molecular box units that compose the polymeric array.

successful outcome of this effort is illustrated by the two nearly isomorphous materials **6** and **7**, obtained from reaction environments containing alcoholic solutions of DMF. Crystals of **6** and **7** consist of two-dimensional coordination polymers, which are sustained by tetranuclear metal ion connectors. The above-described molecular-box motif assembled around crystallographic inversion observed in **4** and **5** is preserved in the polymeric arrays in **6** and **7** as well (Figure 6). However, in the latter DMF (instead of pyridine) acts as an axial ligand to the porphyrin-inserted Cd1 ion. The Cd1-porphyrin molecule is characterized by a domed shape with Cd1 deviating from the four pyrrole N-atoms toward the DMF ligand, and the four carboxylate legs are oriented at the convex side of the molecule.

Figure 6b illustrates the tetranuclear coordination synthon  $\text{Cd}_4(\text{py})_4(\text{MeOH})_2(\text{COO}^-)_8$  in **6** that connects between four neighboring porphyrin dimers/boxes. Each of the metal ions in the tetranuclear cluster bridges between the upper and lower porphyrin in such dimer and further links to the two porphyrin faces of an adjacent dimer. The two metal centers Cd2 and Cd3 are interlinked by two carboxylate groups of two different porphyrin dimers, each one of them coordinating also in a

chelating bidentate manner to another carboxylate moiety. One of the carboxylates of dimers a and d (Figure 6) bridges in a  $\mu^2$ - $\eta^1$ - $\eta^1$  mode between the outer metal ions Cd2 and Cd3, while one of the carboxylates of dimers b and c connects between three metal centers, Cd3, Cd2, and inversion-related Cd2, in a  $\mu^2$ - $\eta^2$ - $\eta^2$  bridging-mode. The coordination sphere of Cd2 includes also one pyridine moiety and that of Cd3 involves one pyridine and one methanol ligand. Around the seven-coordinate Cd2, Cd–O/N coordination distances are within 2.259–2.497(4) Å. Cd3 is six-coordinate to the surrounding ligands at 2.203–2.449(4) Å. The Cd1–N<sub>pyrrole</sub> and Cd1–O<sub>DMF</sub> bonds are 2.186–2.207(5) and 2.349(8) Å, respectively.

In the observed structure every porphyrin-dimer molecular-box is associated with four different tetranuclear connectors (Figure 7). This tetradentate functionality of square-planar topology leads to the formation of bilayered coordination networks that are parallel to the *ac* plane of the crystal. The polymeric arrays pack, in an offset-stacked manner, along the *b*-axis. Additional molecules of the DMF crystallization solvent are trapped in the interstitial voids. The coordination pattern in **7** is identical to that in **6**. However, as **7** was obtained from a

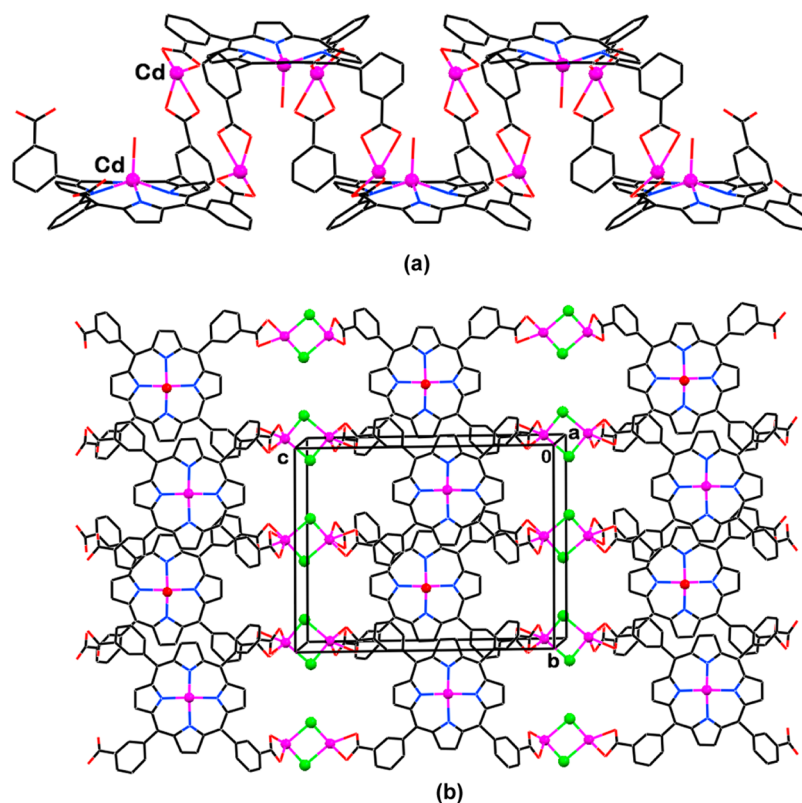


**Figure 8.** (a) The “square-wave” interporphyrin coordination in **8**. The DMF species axially ligated to Cd-ion in the porphyrin center are represented by the metal-bound  $O_{\text{DMF}}$  atom only. The exocyclic Cd-connectors are lined on the periphery of the coordination chains, being exposed to further interchain interaction. (b) Bilayered coordination patterns of the tube-like polymeric metal-porphyrin arrays, extending along the *b*-axis, are joined into a two-dimensional coordination polymer via chloride anions.

pyridine-free environment, in its coordination framework all the auxiliary ligands attached to the Cd2 and Cd3 centers are molecules of DMF, which replace the pyridine species that are attached to these atoms in **6**.

Cadmium chloride as starting material, and  $\text{H}_2\text{O}/\text{DMF}/\text{acetonitrile}$  environment, were used in the synthesis of compound **8**. However, very poorly diffracting crystals could be obtained in this case, and only a preliminary structural model of **8** is available at the present stage. It provided an interesting modification of the coordination pattern, in the sense that the molecular-box motif is not preserved any longer, which may warrant nevertheless a brief discussion of the observed supramolecular architecture. The Cd- $\text{T}^3\text{CPP}$  framework still represents the domed table-like conformer of this organic linker, as in the previous examples **4**–**7**. Yet, the two adjacent inverted “tables” are now shifted with respect to one another so that one pair of carboxylate legs is coordinated through the monomeric cadmium connectors to one neighboring porphyrin, while the second pair of legs is bound via other Cd nodes to the legs of another porphyrin (Figure 8a). This results in the formation of molecular “tubes” (instead of molecular boxes) that propagate in a “square-wave” manner along the *b*-axis of the crystal. The interior of these tubes is filled (in a disordered manner) with the DMF axial ligands bound to the porphyrin metal centers and turned inward.

## CONCLUDING REMARKS

Following the attractively rich supramolecular chemistry of the tetrapyrrolylporphyrin and tetra(carboxyphenyl)porphyrin building blocks,<sup>1–18,21,23</sup> this study reports on some interesting

new structures involving the  $\text{T}^3\text{CPP}$  scaffold. The four *meso*-substituted 3-carboxyphenyl arms of this ligand can assume alternative orientations with the carboxylic sites positioned either above or below the porphyrin macrocycle, leading to different directionalities of the possible intermolecular associations. In our earlier investigations of network assemblies with this organic ligand only the “chairlike” conformer was observed with one pair of *cis*-related carboxyphenyl substituents pointing in one direction and the other pair in the opposite direction.<sup>11</sup> The original aim in the present exploratory investigations was to construct, in view of our earlier observations with the analogous tetra(3-pyridyl)porphyrin moiety,<sup>24,25</sup> framework coordination polymers of diamondoid topology. It has been assumed that reactions of this porphyrin with transition metal ions of preferential tetrahedral coordination environment will induce and stabilize the expression of the “tetrahedral” conformer of the ligand with alternating orientations of adjacent 3-carboxyphenyl groups along the macrocycle and lead to diamondoid coordination frameworks. Such thermodynamically stable systems may sustain open voids for possible utility in gas storage and related sorption/desorption applications. The outcome was quite disappointing in this sense, but it provided also some new structural insights. We failed to formulate framework solids of three-dimensional connectivity in this case. Some of the performed reactions yielded unintentionally hydrogen-bonding networks (in **1**–**3**) instead of the anticipated coordination polymers, revealing the occurrence of the “chair” conformer of the  $\text{T}^3\text{CPP}$  as in the coordination frameworks with lanthanoid ions observed earlier. But then, in coordination compounds with zinc and cadmium

ions which we did obtain, the previously unobserved “table” conformer was solely expressed (in 4–8). Evidently, this isomer of T<sup>3</sup>CPP is not a suitable building block to invoke extended coordination in three dimensions, as its four carboxylic functionalities are oriented roughly in the same directions. On the other hand, it is perfectly suited to form molecular-box-type supramolecular motifs with the aid of exocyclic metal ion connectors, the significant role that porphyrins have played in the synthesis of molecular boxes and cages for various applications being well documented in recent literature.<sup>30–36</sup> In this work 0D, 1D, and 2D hybrid metal-T<sup>3</sup>CPP coordination compounds, in which the diporphyrin molecular-box motif is preserved, have been obtained in crystalline forms. Emergence of new and possibly more robust coordination polymeric solids with the still missing tetrahedral form (wherein the carboxylic substituents are oriented in alternating directions around the porphyrin macrocycle) of this versatile T<sup>3</sup>CPP ligand is to be expected, once the appropriate experimental conditions to this end will be worked out.

## EXPERIMENTAL SECTION

All starting reagents and reagent-grade solvents (Aldrich, Merck) were procured commercially and used without further purification. The 5,10,15,20-tetrakis(3-carboxyphenyl)porphyrin (T<sup>3</sup>CPP) was synthesized by the modified Lindsey method,<sup>26</sup> involving KOH hydrolysis of the corresponding carbomethoxyphenyl intermediate.<sup>21</sup>

**The Porphyrin Synthesis.** Thus, 2 g (0.123 mol) of 3-carbomethoxybenzaldehyde and 0.85 mL of distilled pyrrole (0.123 mol) were added to 700 mL of dry CH<sub>2</sub>Cl<sub>2</sub> and purged with argon for 30 min. Then, BF<sub>3</sub> etherate (0.4 mL, 3.16 mmol) was added via syringe, and the reaction mixture was protected from light. After stirring at room temperature for 1 h, 2.3 g (9.35 mmol) of *p*-chloranil was added in the solid form and the solution was stirred overnight. The solution was concentrated to a small volume using a rotary evaporator. To this solution, silica gel (60–200 mesh) was added and the slurry was evaporated to give a dry black powder, which was loaded on a silica column using CHCl<sub>3</sub>. First CHCl<sub>3</sub> fraction removed any poly(pyrrole) impurity and the porphyrin was eluted with 2–4% acetone in CHCl<sub>3</sub>. It was then further purified by recrystallization from a 1:4 CHCl<sub>3</sub>/methanol mixture (v/v). Yield: 0.48 g (18.6%). In the next stage, 0.25 g (0.295 mmol) of the latter product was dissolved in 40 mL of THF. To this, 1.65 g (0.0295 mol) of KOH in 1 mL of water was added and the solution was heated at 75 °C for 16 h. At the end of this period, THF was removed by rotary evaporation. The crude porphyrin was treated with 30 mL of 2 N HCl solution, yielding a green precipitate, which was filtered, washed with water, and dried. Protonated porphyrin was neutralized by adding 10 mL of pyridine and subsequently removed by vacuum distillation. Then, purple solid was washed with water and dried under a vacuum. Yield: 0.21 g (88%).

**Supramolecular Syntheses and Crystallization Procedures.** The supramolecular crystalline assemblies were obtained by the following procedures:

1. T<sup>3</sup>CPP (0.010 mmol) and cadmium(II) chloride (0.031 mmol) were placed in a sealed reactor with H<sub>2</sub>O/DMF (1:1, 2 mL) solution and added 3 drops of concentrated HCl. Green precipitate was formed. The reactor was heated to 150 °C for 3 days in a dry bath. Then, the temperature was decreased to 120 °C for an additional 24 h. After slow cooling, X-ray quality purple very small needle crystals were obtained (yield 95% based on porphyrin).
2. T<sup>3</sup>CPP (0.007 mmol) and cadmium(II) chloride (0.008 mmol) were placed in sealed reactor with DMF/ethanol (1:1, 2 mL) solution and 1 drop of DBU (1,8-diazabicyclo[5.4.0]undec-7-ene) was added. The sealed vial was heated to 85 °C for 3 days in a dry bath. After slow cooling, X-ray quality small red crystals were obtained (yield 90% based on porphyrin).

3. T<sup>3</sup>CPP (0.007 mmol) and cobalt(II) chloride (0.016 mmol) were placed in sealed reactor with H<sub>2</sub>O/DMF (2:1, 2 mL) solution and 3 drops of ammonium hydroxide 25% were added. The sealed vial was heated to 100 °C for 3 days in a dry bath. After slow cooling, X-ray quality red crystals were obtained (yield 8% based on porphyrin).
4. T<sup>3</sup>CPP (0.006 mmol) and cadmium(II) nitrate (0.019 mmol) were placed in a sealed reactor with pyridine and methanol (1:1, 2 mL) solution. The reactor was heated to 80 °C for 3 days in a dry bath. Cooling of the vessel to room temperature yielded clear red solution. One milliliter of DMSO was added to the reactor; it was sealed again and heated to 120 °C for 3 additional days. Slow cooling of the vial to ambient conditions yielded two kinds of crystals: X-ray quality purple crystals (yield ~ 4% based on porphyrin) as well as red air-sensitive crystals that transform rapidly to amorphous material.
5. T<sup>3</sup>CPP (0.009 mmol) and zinc(II) chloride (0.037 mmol) were placed in a vial with ethanol/DMF (2:1, 2 mL) solution. The sealed vial was heated to 100 °C for 3 days in a dry bath. After slow cooling to room temperature, very small, polycrystalline material was obtained. Then, 1 mL of pyridine was added to the vial, which was sealed again and heated to 80 °C for 3 additional days. After slow cooling, X-ray quality red needle crystals were obtained (yield ~ 5% based on porphyrin). The same crystals were prepared from the reaction of zinc(II) nitrate (0.020 mmol) with the T<sup>3</sup>CPP.
6. T<sup>3</sup>CPP (0.007 mmol) and cadmium(II) nitrate (0.017 mmol) (were placed in sealed reactor with pyridine, DMF, and methanol (1:1:1, 2 mL) solution. The sealed vial was heated to 80 °C for 3 days in a dry bath. After slow cooling, X-ray quality red crystals were obtained (yield 90% based on porphyrin).
7. T<sup>3</sup>CPP (0.007 mmol) and cadmium(II) chloride (0.020 mmol) were placed in sealed reactor with DMF and ethanol or methanol (1:1, 2 mL) solution. The sealed vial was heated to 80 °C for 3 days in a dry bath. After slow cooling, X-ray quality red crystals were obtained (yield 85% based on porphyrin).
8. T<sup>3</sup>CPP (0.006 mmol) and cadmium(II) chloride (0.017 mmol) were placed in vial with H<sub>2</sub>O/DMF (2:1, 2 mL) solution and covered with 1 mL of acetonitrile. The sealed vial was heated to 80 °C for 3 days in a dry bath. After slow cooling, X-ray quality red very flat cube poorly diffracting crystals were obtained (yield ~ 5% based on porphyrin). The same poor-quality crystals were prepared from the reaction of cadmium(II) nitrate (0.032 mmol) with the T<sup>3</sup>CPP in similar experimental conditions.

The uniform identity of the formed crystal lattices (1–8) in a given reaction was confirmed in each case by repeated measurements of the unit-cell dimensions from different randomly chosen single crystallites. Because of deterioration of several of the crystalline products (prepared in milligram-scale amounts) when taken out from the crystallization solution and/or during the drying process (in particular, 4, 5, and 8), elemental analysis and powder diffraction experiments could not be carried out reliably in a systematic manner. For their structure determination crystals pulled out from the reaction vials were covered immediately by protective oil and cooled down to 100–120 K on the diffractometer. The composition of the respective solids were determined by crystallography: **1:** (T<sup>3</sup>CPP)<sup>2-</sup>·2(CH<sub>3</sub>NH<sub>2</sub>CH<sub>3</sub>)<sup>+</sup>; **2:** (T<sup>3</sup>CPP)<sup>2-</sup>·2(DBU-H)<sup>+</sup>; **3:** (Co-T<sup>3</sup>CPP)<sup>4-</sup>·2(CH<sub>3</sub>NH<sub>2</sub>CH<sub>3</sub>)<sup>+</sup>·2(NH<sub>4</sub>)<sup>+</sup>; **4:** {[Cd(py)<sub>3</sub>T<sup>3</sup>CPP]<sup>4-</sup>·[Cd(py)<sub>2</sub>(H<sub>2</sub>O)]<sup>4+</sup>}]<sub>2</sub>·S [S = 4(py)·2(MeOH); noncoordinated crystallization solvent, where py = pyridine]; **5:** {[Zn(py)T<sup>3</sup>CPP]<sup>4-</sup>·[Zn(py)<sub>2</sub>Zn(py)]<sup>4+</sup>}]<sub>2</sub>·S [S = x(py)·y(MeOH), a mixture of disordered pyridine and methanol as crystallization solvent of uncertain content trapped in the crystal lattice]; **6:** {[Cd(DMF)T<sup>3</sup>CPP]<sup>4-</sup>·[Cd(py)(MeOH)Cd(py)]<sup>4+</sup>}]<sub>n</sub>·(0.66DMF)<sub>n</sub>; **7:** {[Cd(DMF)T<sup>3</sup>CPP]<sup>4-</sup>·[Cd(DMF)(MeOH)Cd(DMF)]<sup>4+</sup>}]<sub>n</sub>·(xDMF)<sub>n</sub>; **8:** {[Cd(DMF)T<sup>3</sup>CPP]<sup>4-</sup>·4·(CdCl)<sup>+</sup>}]<sub>n</sub>·(xDMF)<sub>n</sub>.

**Crystallography.** The X-ray measurements [Bruker X8-Prosppector, CuKα radiation (1); Bruker-ApexDuo (2) and Nonius-

KappaCCD (3–8) diffractometer, MoK $\alpha$  radiation) were carried out at ca. 100 K (1), 120 K (2), and 110 K (3–8) on crystals coated with a thin layer of amorphous oil to minimize crystal deterioration, possible structural disorder and related thermal motion effects, and to optimize the precision of the structural results. These structures were solved by direct methods and refined by full-matrix least-squares (SIR-97 and SHELXL-97).<sup>27,28</sup> All non-hydrogen atoms were refined anisotropically. The hydrogen atoms were located in idealized/calculated positions and were refined using a riding model; most of those involved in hydrogen bonds were located directly in difference-Fourier maps but were not refined. The crystallographic refinements of structures 1–4 and 6 converged smoothly to relatively low *R*-values. Compounds 5 and 7 were found to contain disordered crystallization solvent (pyridine and methanol in 5 and DMF in 7). The solvent species could be clearly recognized in difference electron-density maps, but could not be reliably modeled by discrete atoms due to their severe disorder in the interstitial voids. Correspondingly, the contribution of the disordered solvent moieties in 5 and 7 was subtracted from the diffraction pattern by the SQUEEZE procedure and PLATON software.<sup>29</sup> Crystals of compound 8 diffracted very poorly and at low-resolution. Correspondingly, only preliminary structural model (excluding the disordered solvent) could be obtained at this stage from the limited experimental diffraction data. It is presented here, nevertheless, due to the unique coordination scheme it reveals with the table-like conformer of the T<sup>3</sup>CPP.

## ■ ASSOCIATED CONTENT

### 📄 Supporting Information

X-ray crystallographic files in CIF format for the eight analyzed crystalline solids 1–8. This information is available free of charge via the Internet at <http://pubs.acs.org>

## ■ AUTHOR INFORMATION

### Corresponding Author

\*Tel.: +972-3-6409965; fax: +972-3-6409293; e-mail: [goldberg@post.tau.ac.il](mailto:goldberg@post.tau.ac.il)

### Notes

The authors declare no competing financial interest.

## ■ ACKNOWLEDGMENTS

This research was supported by The Israel Science Foundation (Grants No. 502/08 and 108/12). The authors are grateful to Dr. Holger Ott (Bruker-Axs) for the laborious data collection of compound 1.

## ■ REFERENCES

- (1) Dastidar, P.; Stein, Z.; Goldberg, I.; Strouse, C. E. *Supramol. Chem.* **1996**, *7*, 257–270.
- (2) Diskin-Posner, Y.; Goldberg, I. *J. Chem. Soc., Chem. Commun.* **1999**, 1961–1962.
- (3) Diskin-Posner, Y.; Dahal, S.; Goldberg, I. *J. Chem. Soc., Chem. Commun.* **2000**, 585–586.
- (4) Diskin-Posner, Y.; Dahal, S.; Goldberg, I. *Angew. Chem., Int. Ed.* **2000**, *39*, 1288–1292; *Angew. Chem.* **2000**, *112*, 1344–1348.
- (5) Kosal, M. E.; Chou, J.-H.; Wilson, S. R.; Suslick, K. S. *Nat. Chem.* **2002**, *1*, 118–121.
- (6) Smithenry, D. W.; Wilson, S. R.; Suslick, K. S. *Inorg. Chem.* **2003**, *42*, 7719–7721.
- (7) Suslick, K. S.; Bhyrappa, P.; Chou, J. H.; Kosal, M. E.; Nakagaki, S.; Smithenry, D. W.; Wilson, S. R. *Acc. Chem. Res.* **2005**, *38*, 283–291.
- (8) Goldberg, I. *Chem.—Eur. J.* **2000**, *6*, 3863–3870.
- (9) Goldberg, I. *Chem. Commun.* **2005**, 1243–1254.
- (10) Goldberg, I. *CrystEngComm* **2008**, *10*, 637–645.
- (11) Lipstman, S.; Muniappan, S.; George, S.; Goldberg, I. *Dalton Trans.* **2007**, 3273–3281.
- (12) Choi, E.-Y.; Barron, M. B.; Novotny, R. W.; Son, H.-T.; Hu, Ch.; Choe, W. *Inorg. Chem.* **2009**, *48*, 426–428.
- (13) Barron, M. B.; Son, H.-T.; Hu, Ch.; Choe, W. *Cryst. Growth Des.* **2009**, *9*, 1960–1965.
- (14) Barron, M. B.; Wray, C. A.; Hu, Ch.; Guo, Z.; Choe, W. *Inorg. Chem.* **2010**, *49*, 10217–10219.
- (15) Burnet, B. J.; Barron, M. B.; Hu, Ch.; Choe, W. *J. Am. Chem. Soc.* **2011**, *133*, 9984–9987.
- (16) Burnet, B. J.; Barron, M. B.; Choe, W. *CrystEngComm* **2012**, *14*, 3839–3846.
- (17) Fateeva, A.; Chater, P. A.; Ireland, C. P.; Tahir, A. A.; Khimyak, Y. Z.; Wiper, P. V.; Darwent, J. R.; Rosseinsky, M. J. *Angew. Chem., Int. Ed.* **2012**, *51*, 7440–7444.
- (18) Motoyama, S.; Makiura, R.; Sakata, O.; Kitagawa, H. *J. Am. Chem. Soc.* **2011**, *133*, 5640–5643.
- (19) Meng, L.; Cheng, Q.; Kim, C.; Gao, W.-Y.; Wojtas, L.; Chen, Y.-S.; Zaworotko, M. J.; Zhang, X. P.; Ma, S. *Angew. Chem., Int. Ed.* **2012**, *51*, 10082–10085.
- (20) Wang, X.-S.; Chrzanowski, M.; Gao, W.-Y.; Wojtas, L.; Chen, Y.-S.; Zaworotko, M. J.; Ma, S. *Chem. Sci.* **2012**, *3*, 2823–2827.
- (21) Muniappan, S.; Lipstman, S.; George, S.; Goldberg, I. *Inorg. Chem.* **2007**, *46*, 5544–5554.
- (22) Burrows, A. D.; Cassar, K.; Friend, R. M. W.; Mahon, M. F.; Rigby, S. P.; Warren, J. E. *CrystEngComm* **2005**, *7*, 548–550.
- (23) DeVries, L. D.; Choe, W. *J. Chem. Crystallogr.* **2009**, *39*, 229–240.
- (24) Lipstman, S.; Goldberg, I. *Cryst. Growth Des.* **2010**, *10*, 4596–4606.
- (25) Lipstman, S.; Goldberg, I. *Cryst. Growth Des.* **2010**, *10*, 5001–5006.
- (26) Lindsey, J. S.; Schreiman, I. C.; Hsu, H. C.; Kearney, P. C.; Margueretaz, A. M. *J. Org. Chem.* **1987**, *52*, 827–836.
- (27) Altomare, A.; Burla, M. C.; Camalli, M.; Casciaro, M.; Giacovazzo, C.; Guagliardi, A.; Polidori, G. *J. Appl. Crystallogr.* **1994**, *27*, 435–436.
- (28) Sheldrick, G. M. *Acta Crystallogr.* **2008**, *A64*, 112–122.
- (29) Spek, A., L. *J. Appl. Crystallogr.* **2003**, *36*, 7–13.
- (30) Chamberon, J.-C.; Heitz, V.; Sauvage, J.-P. *The Porphyrin Handbook*; Guillard, R.; Smith, K. M.; Kadish, K. M., Eds.; Academic Press: New York, 2000; Vol. 1, pp. 1–42.
- (31) Fujita, M.; Tominaga, M.; Hori, A.; Therrien, B. *Acc. Chem. Res.* **2005**, *38*, 371–380.
- (32) Lee, S. J.; Hupp, J. T. *Coord. Chem. Rev.* **2006**, *250*, 1710–1723.
- (33) Stultz, E.; Scott, S. M.; Bond, A. D.; Teat, S. J.; Sanders, J. K. M. *Chem.—Eur. J.* **2003**, *9*, 6039–6048.
- (34) Hwang, I.-W.; Kamada, T.; Ahn, T. K.; Ko, D. M.; Nakamura, T.; Tsuda, A.; Osuka, A.; Kim, D. *J. Am. Chem. Soc.* **2004**, *126*, 16187–16198.
- (35) Zhang, J.; Li, Y.; Yang, W.; Lai, S.-W.; Zhou, C.; Liu, H.; Che, C.-M.; Li, Y. *Chem. Commun.* **2012**, *48*, 3602–3604.
- (36) Wang, X.-S.; Heng, L.; Cheng, Q.; Kim, C.; Wojtas, L.; Chrzanowski, M.; Chen, Y.-S.; Zhang, X. P.; Ma, S. *J. Am. Chem. Soc.* **2011**, *133*, 16322–16325.